

OPTIMIZATION OF THE GATING SYSTEM FOR SAND CASTING USING GENETIC ALGORITHM

Nedeljko Dučić, Radomir Slavković, and Ivan Milićević

Faculty of Technical Sciences Čačak, University of Kragujevac, Svetog Save 65, 32000 Čačak, Serbia

Žarko Čojbašić

Faculty of Mechanical Engineering, University of Niš, Aleksandra Medvedeva 14, 18000 Niš, Serbia

Srećko Manasijević and Radomir Radiša

Lola Institute, Kneza Višeslava 70a, 11030 Belgrade, Serbia

Copyright © 2016 American Foundry Society
DOI 10.1007/s40962-016-0040-8

Abstract

The paper presents a methodology of optimization of the gating system for sand casting using the genetic algorithm. Software package for computer-aided design/computer-aided manufacturing (CAD/CAM) was used as the support to the design and verification of the optimized gating system. The geometry of the gating system of sand casting in excavator tooth holder was the subject of optimization. The objective was to maximize filling rate given the constraints posed by both the ingate module and Reynolds number. Mold filling time has been presented as

a function of the ingate cross section and casting height. Given the conditions above, as the result of the optimization, a complete geometry of the gating system has been defined. Numerical simulation (software MAGMA⁵) has been used to verify the validity of the optimized geometry of the gating system.

Keywords: genetic algorithm, numerical simulation, gating system, optimization, sand casting

Introduction

Proper and complete mold filling is the main objective of the sand casting process which ensures high quality of the casting part. To this end, the design of the gating system is of major importance, as improper designing of the system results in a number of defects in the casting process. The defects include incomplete filling, inclusions and gaseous entrapments. Incomplete filling is manifested in two forms: cold shut or misrun. A cold shut occurs when two fluids running in opposite directions meet and fail to fully merge, whereas a misrun occurs when molten metal fails to fill in particular parts of the mold. Inclusions are the direct result of turbulence, being manifested as sand inclusion. Gaseous entrapments occur in the form of the air 'trapped' in the mold, in the form of blow hole and gas porosity. Therefore, the gating system aims at providing a smooth, uniform and complete filling of the mold with pure, molten metal. Smooth filling eliminates turbulence, and uniform filling

ensures continuous mold filling, whereas complete filling allows the molten metal to reach minor, end cavities of the mold.

Optimization of the casting process has been the subject of numerous studies performed so far. Approaches to the studies aimed at improving the casting process are numerous. They differ in parameters to be optimized and in optimization techniques applied. Jacob et al.¹ presented the integration of genetic algorithm (GA) and computer-aided design (CAD) in the design and optimization of feeders in the casting process. Masoumi et al.² investigated the effects of gating design including gate geometry and size on the flow pattern by pouring molten metal of aluminum alloy A413 into a sand mold. Esparza et al.³ presented a numerical optimization technique based on gradient search, for obtaining an optimal design of a typical gating system used for the gravity process to produce aluminum parts. In their attempts to improve quality of the cast, Guharaja

et al.⁴ optimized significant parameters of the green sand casting process by using the Taguchi's method, Tavakoli and Davami⁵ focused on the design of the feeding system in sand casting process using the SIMP method. Sun et al.⁶ presented the optimization of the four gating system parameters. Namely, ingate height, ingate width, runner height and runner width were optimized with consideration of multiple performance characteristics including filling velocity, shrinkage porosity and product yield. Different magnesium alloys have been employed to illustrate the effectiveness of this approach.⁶ Kor et al.⁷ proposed an optimization of the gating and riser design of the sand casting, formulated as a multi-objective optimization problem with conflicting objectives and a complex search space. Kotas et al.⁸ summarized the findings of multi-objective optimization of a gravity sand-cast steel part for which an increase in casting yield via riser optimization was considered. Shinde et al.⁹ proposed a methodology to optimize mold yield by selecting the correct combination of the mold box size and the number of cavities based on solidification time and mold temperature, whereas Kumaravadivel and Natarajan¹⁰ optimized the process variables in sand casting. In this research, the authors have kept their prime focus on minimizing the defects developed in the sand casting process by PWA (process window approach).¹⁰ Oji et al.¹¹ presented optimization of process parameters in sand casting as a function of mechanical properties of the cast part. Surekh et al.¹² presented a multi-objective optimization of green sand mold system using evolutionary algorithms, such as GA and particle swarm optimization (PSO). In this study, nonlinear regression equations developed between the control factors (process parameters) and responses like green compression strength, permeability, hardness and bulk density have been considered for optimization utilizing GA and PSO.¹²

Presented studies do not provide work based on maximizing the filling rate of molten metal in the casting cavity. Maximum filling rate is critical in thin and long castings which lose heat very rapidly, and higher filling rate helps to avoid defects like cold shuts and misruns. Methodology of feeder definition and design was presented alongside the optimization of the gating system. CAD software supported the optimization with respect to the design and geometry analysis of the casting part, whereas the CAM software was applied for numerical simulation of casting.

Gating System Setup

The casting is part of excavator buckets, i.e., holder of the cutting tooth (its CAD model is shown in Figure 1). The proposed holder of the cutting tooth is made of manganese steel (0.5 % C, 1.4 % Mn, 0.035 % P, 0.035 % S, 0.4 % Si, 0.1 % V) which is able to successfully overcome the dynamic loads and shocks. Casting part dimensions are 295 mm × 320 mm × 90 mm, while the net mass is 25.6 kg.

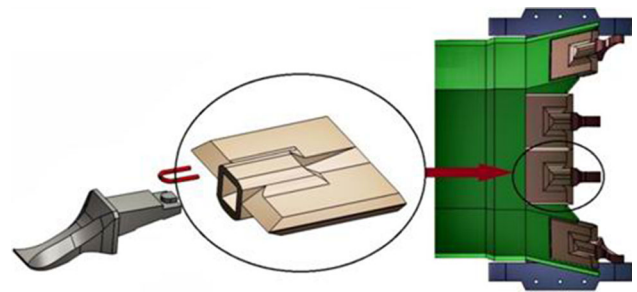


Figure 1. CAD models: cutting tooth, holder of cutting tooth and entire excavator bucket.

The first step of the optimization and design of the gating system is to choose the type of gating system. Depending on its orientation relative to the dividing plane, gating systems can be classified as vertical or horizontal. The first classification includes the ingate position. Gating systems can be classified as top, parting line and/or bottom. Given the first criterion of classification, the horizontal gating system was chosen for its favorable applicability in gravitational sand casting.

The parting-line gating system was opted for with regard to the second criterion. Compared to the bottom gating system, the parting-line gating system has a higher rate of mold filling. Compared to the top gating system, the parting-line gating system yields lower turbulence. Figure 2 shows the proposed gating system, along with the parameters that are the immediate subject of the optimization, i.e., A_{ingate} —ingate cross section area, h_{ingate} —height

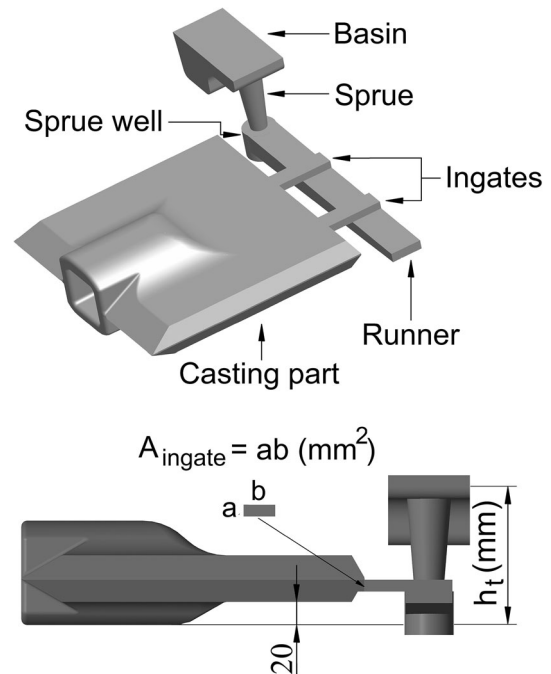


Figure 2. Gating system for casting of holder of cutting tooth.

between the bottom surface of the casting part and the level of molten metal in a basin. Based on the parameters above, the geometrical values of other elements of the gating system were defined.

The proposed gating system includes the pouring basin, sprue, sprue well, runner and ingate—elements of the path from the ladle and all through to the mold cavity. The pouring basin is located on top of the gating system. Its function is to direct the molten metal from the ladle into the sprue. It needs to be deep enough to prevent vortices. The sprue connects the pouring basin and runner. It commonly tapers from pouring basin to prevent aspiration of air from occurring. The sprue well is located at the end of the sprue. It receives the molten metal from the sprue and drives it perpendicularly to the runner. The runner controls speed if this is the choke and delivers the molten metal to the ingate. Finally, ingates connect the runner to the mold cavity. They can have square, rectangular and trapezoidal form, cross-sectionally. In the proposed setup of the gating system, ingates have rectangular cross section.

Optimization of Gating System Geometry

Good casting quality is initially dependent on a good gating design. Foundries tend to replace the design of the gating system and feeders, based on the trial-and-error principle. This part of the paper presents the application of GA aiming to optimize the geometry of the gating system. The primary goal of the optimization is to maximize the filling rate of the mold cavity, within the predefined constraints. The constraints for optimization are specified in the form of modulus of ingate (with respect to the connected section) and Reynolds number.

Genetic algorithms (GAs) are a family of adaptive search algorithms described and analyzed in references.^{13–17} GAs derive their name from the fact that they are loosely based on models of genetic change in a population of individuals. These models consist of three basic elements: (1) a Darwinian notion of ‘fitness,’ which governs the extent to which an individual can influence future generations; (2) a ‘mating operator,’ which produces offspring for the next generation; and (3) ‘genetic operators,’ which determine the genetic makeup of offspring from the genetic material of the parents (Figure 3).¹⁶

Fitness Function

Defining the fitness function is one of the major steps of optimization via GA. The aim of the optimization is to maximize the filling rate (1):

$$\text{Filling_rate} = \rho_m A_{\text{ingate}} V_{\text{ingate}} \quad \text{Eqn. 1}$$

where ρ_m —density of molten metal, A_{ingate} —cross-sectional area of ingate and V_{ingate} —velocity of molten

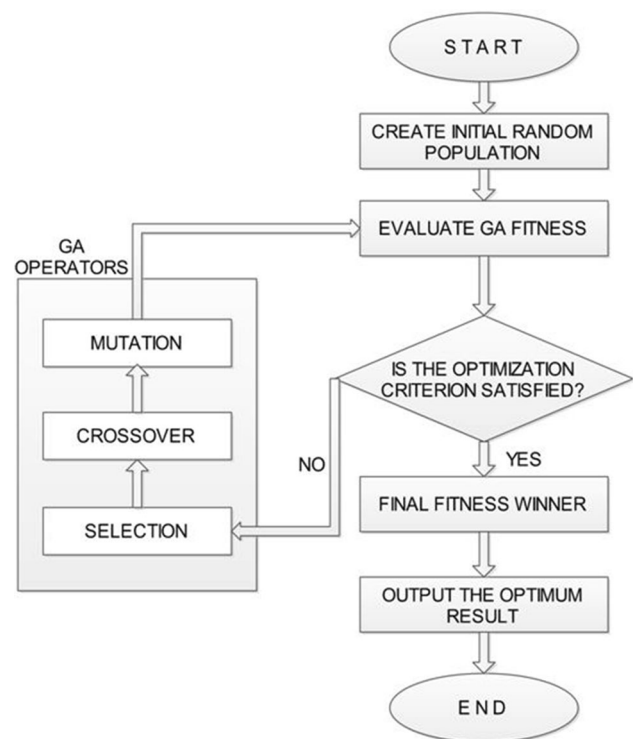


Figure 3. The operation of GA.

metal at ingate. Given the minor variations in density of the metal above the melting point, $\rho_m = \text{const.}$ in this analysis. Thus, filling rate of the mold cavity depends on cross-sectional area of ingate (A_{ingate}) and velocity of molten metal at ingate (V_{ingate}). The increase in filling rate of the mold cavity implies shorter filling time of mold cavity. Hence, minimizing the filling time given in Eqn. (2) is the fitness function and the optimization objective. The total time to fill the mold cavity can be determined by integrating the incremental time of filling for all layers from the bottom to the top of the mold cavity.¹⁸

$$\tau_f = \int_0^{h_{\text{cast}}} \frac{A_i(h)}{\sum_j A_{\text{ingate}-j} \cdot V_{\text{ingate}-j}} dh \quad \text{Eqn. 2}$$

where $A_i(h)$ is the cross-sectional area of the casting layer being filled, $A_{\text{ingate}-j}$ and $V_{\text{ingate}-j}$ are the cross-sectional area and the instantaneous velocity, respectively, of ingate j , and h_{cast} is casting part height, its value being 90 mm. As the two ingates have identical cross sections, $A_{\text{ingate}} = a \cdot b$ and velocity $V_{\text{ingate}} = \sqrt{2g \cdot (h_t - h)}$ yield Eqn. (3).

$$\tau_f = \frac{1}{2ab\sqrt{2g}} \int_0^{h_{\text{cast}}} \frac{A_i(h)}{\sqrt{h_t - h}} dh \quad \text{Eqn. 3}$$

where g —acceleration due to gravity, h_t —distance between the bottom of the casting part and the level of molten metal in the pouring basin (Figure 2). Cross section of the $A_i(h)$ casting part varies, depending on the casting part height. Calculating functions $A_i(h)$ is the next

assignment aimed at obtaining the fitness function. Devising cross sections (whereby $\Delta h = 1$ mm) on the CAD model of the casting part gave area cross section values at respective casting part height (Figure 4; Table 1). Interpolation of the values, obtained by using the three polynomials within appropriate range, resulted in change in cross section relative to casting part height. The first polynomial represents a change in cross section in the range from 0 to 21 mm. Figure 5 shows the graph of the function (4).

$$A_i(0 - 21) = 0.39h^3 - 33.9h^2 + 1095h + 7032 \quad \text{Eqn. 4}$$

The second polynomial represents a change in cross section in the range from 21 to 60 mm (Figure 6).

$$A_i(21 - 60) = 0.1h^4 - 16h^3 - 884.84h^2 + 19285h + 20672.2 \quad \text{Eqn. 5}$$

Finally, the third polynomial represents a change in cross section in the range from 60 to 90 mm (Figure 7).

$$A_i(60 - 90) = 1.7h^3 + 381.89h^2 - 28576h + 731728.18 \quad \text{Eqn. 6}$$

Incorporating polynomials standing for the change in cross section relative to casting part height into relation (3) yielded Eqn. (7).

$$\tau_f = \frac{1}{2ab\sqrt{2g}} \left(\int_0^{21} \frac{A_i(0 - 21)}{\sqrt{h_t - h}} dh + \int_{21}^{60} \frac{A_i(21 - 60)}{\sqrt{h_t - h}} dh + \int_{60}^{90} \frac{A_i(60 - 90)}{\sqrt{h_t - h}} dh \right) \quad \text{Eqn. 7}$$

Solving each integral individually and retrieving the solutions into (7) yielded the final expression of fitness functions (8).

$$\tau_f = \frac{I_1(h_t) + I_2(h_t) + I_3(h_t)}{2ab\sqrt{2g}} \quad \text{Eqn. 8}$$



Figure 4. Area cross section of casting part A_i (52 mm) = 78,041.27 mm².

Table 1. Some of the Values of Cross-Sectional Area

h (mm)	A (mm ²)	h (mm)	A (mm ²)	h (mm)	A (mm ²)
0	6077.58	48	80,138.21	84	8977.42
1	8575.50	49	79,605.98	85	8340.68
2	9627.27	50	79,079.07	86	7638.00
3	10,444.50	51	78,557.51	87	6845.75
4	11,111.12	52	78,041.27	88	5922.57
5	11,679.46	53	77,530.37	89	4760.36
6	12,184.11	54	77,025.96	90	2230.27
...

Defining Constraints

Modulus of Ingate

This constraint was defined by the relation (9). Ingate module needs to be lower than or equal to the casting part module.

$$\left\{ \begin{array}{l} M_{\text{ingate}} \leq M_{\text{casting_part}} \\ \left(\frac{A_{\text{ingate}}}{P_{\text{ingate}}} \right) \leq \left(\frac{V_{\text{casting_part}}}{A_{\text{casting_part}}} \right) \end{array} \right\} \quad \text{Eqn. 9}$$

where n —ingate number, A_{ingate} —ingate cross section, P_{ingate} —perimeter of ingate, $V_{\text{casting_part}}$ —casting part volume and $A_{\text{casting_part}}$ —surface area of casting part. Two ingates are foreseen, while the analysis of the CAD model gave: $V_{\text{casting_part}} = 3661113.8$ mm³ and $A_{\text{casting_part}} = 253716.66$ mm². Cross section and perimeter are: $A_{\text{ingate}} = ab$, $P_{\text{ingate}} = 2(a + b)$.

The incorporation of the values above into Eqn. (9) yielded the final constraint form given by Eqn. (10).

$$ab - 14.43 \cdot (a + b) \leq 0 \quad \text{Eqn. 10}$$

Reynolds Number

When the flow takes place in a closed channel, i.e., when the fluid is completely bounded by solid faces and the flow is incompressible, the Reynolds number can be used to describe the flow. The Reynolds number is the ratio between the inertia forces and the viscous forces. The inertia forces are a measure for the tendency of the flow to move in the direction of the momentum in the flow; the viscous forces are trying to counteract this motion, due to viscous drag from the side walls of the channel containing the flow, i.e., it is a balance between dynamic forces and braking shear forces from viscosity. The Reynolds number is given by (11).¹⁹

$$Re = \frac{\text{Inertia_forces}}{\text{Viscous_forces}} = \frac{\rho V_{\text{ingate}} d}{\mu} \quad \text{Eqn. 11}$$

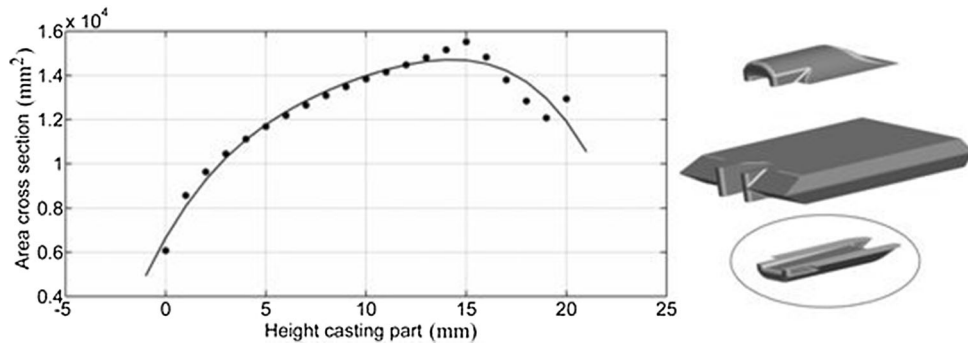


Figure 5. Graph showing function A_i (0–21).

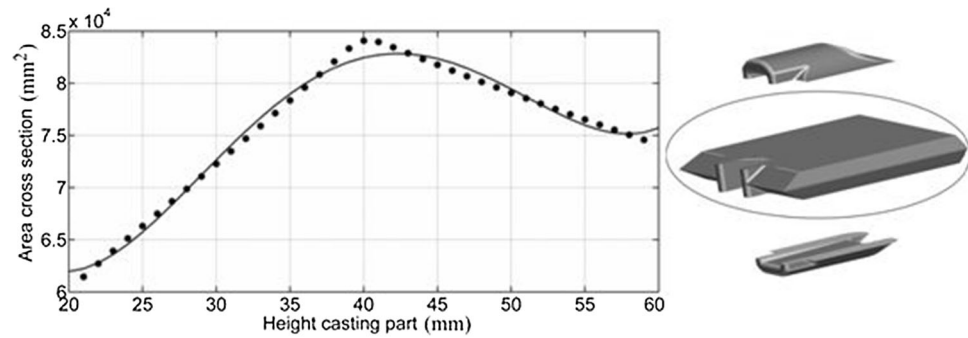


Figure 6. Graph showing function A_i (21–60).

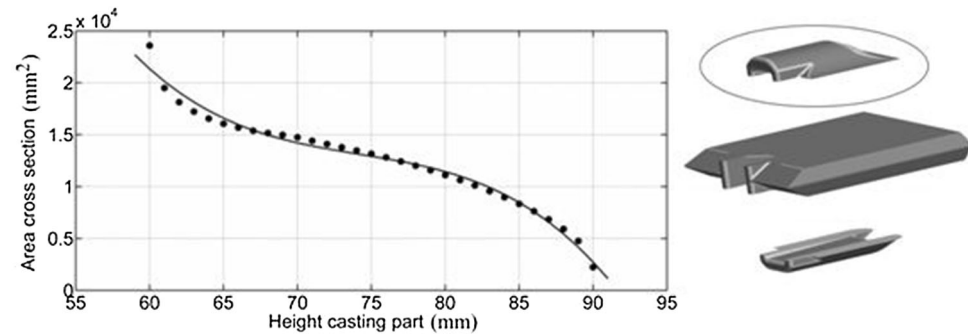


Figure 7. Graph showing function A_i (60–90).

where μ —dynamic viscosity of molten metal, d —characteristic length, given by Eqn. (12).

$$d = \frac{4A_{\text{ingate}}}{P_{\text{ingate}}} = \frac{4ab}{2(a+b)} = 2 \frac{ab}{a+b} \quad \text{Eqn. 12}$$

A high Reynolds number leads to turbulent flow. So in order to avoid highly turbulent flow, the Reynolds number should be less than 20,000.¹⁹ Given the fact, (11) and (12) result in Eqn. (13). The Reynolds number (13) was chosen to be the moment of the first contact between the molten metal and mold, i.e., 20 mm from the bottom of the casting part (Figure 2).

$$Re = 2 \frac{\rho}{\mu} \sqrt{2g} \frac{ab\sqrt{h_t - 20}}{a+b} \leq 20,000 \quad \text{Eqn. 13}$$

Viscosity of steel is $\mu = 7 \times 10^{-3}$ kg/ms, and density is $\rho = 7000$ kg/m³. Incorporating the values above into (13) yields the final constraint Eqn. (14).

$$ab\sqrt{h_t - 20} - 71.4(a+b) \leq 0 \quad \text{Eqn. 14}$$

Optimization Results

Search domain of size values that are being optimized is given in Table 2. The upper and lower limits are set in accordance with the proposed geometry of the gating system.

The population range is 120 individuals, with 50 generations at maximum. Stochastic universal sampling algorithm

is used in the selection. The population is seen as mapped on the roulette wheel, larger parts of the wheel belonging to strings with lower fitness (since it is a minimization problem). N pointers are evenly placed on the roulette, N being the number of individuals in a population. A population is generated by rotating the roulette once. As the operator of the crossing was used uniform crossover. The coefficient of the 'crossover fraction' is 0.8. Crossover fraction defines a portion of the new population derived from a crossing (non-elite individuals), its value being between 0 and 1. Not more than two elite individuals are to be transferred to the next generation. The operation of GA is terminated as early as the fifth generation due to the violation of specified limits. Fitness function values which represent the minimized time of mold filling are $\tau_f = 5.75$ s. The obtained optimized values are as follows: $h_t = 110.53$ mm, $a = 10$ mm and $b = 29.98$ mm; therefore, $A_{\text{ingate}} = 300$ mm², and $h_t = 110$ mm are the values which will determine the entire gating system (Figure 8).

The optimization results (ingate size and casting height) give the overall geometry of the gating system. To set off designing elements of the gating system, besides the value of ingate cross section, it is necessary to opt for one of the two filling systems. In 1954, the renowned researchers Johnson, Bishop and Pellini classified the filling systems as pressurized and unpressurized. In our paper, the former was opted for. Pressurized and unpressurized systems differ in selection of the choke which controls flow of the melted metal through the gating system. In the pressurized running system, the metal flow is choked (i.e., limited by constriction) at the gate, i.e., its rate of flow into the mold is controlled by the gate area, which is the final point in the running system.²⁰

Both filling systems are characterized by correlated cross sections of the sprue exit, runner and ingate. Campbell²⁰ gave two recommendations regarding the pressurized system, i.e., sprue exit/runner area/ingate area = 1:0.8:0.6 and sprue exit/runner area/ingate area = 1:1:0.8. Based on the ingate area ($A_{\text{ingate}} = 300$ mm²) and applying the first recommendation, runner area and sprue exit were determined at $A_{\text{runner}} = 400$ mm² and $A_{\text{sprue}} = 500$ mm², respectively. A tapered runner allows uniform filling of the ingate at relatively similar speed.²⁰ The sprue is circular in cross section due to the small surface area exposed to cooling and lower resistance to flow of the metal. Dimensions of the sprue well were defined based on the dimension of the runner and sprue, i.e., the elements of gating system directly connected with the sprue well. The

Table 2. Optimal Values Search Domain

	a (mm)	b (mm)	h_t (mm)
Lower bound	10	10	100
Upper bound	30	30	130

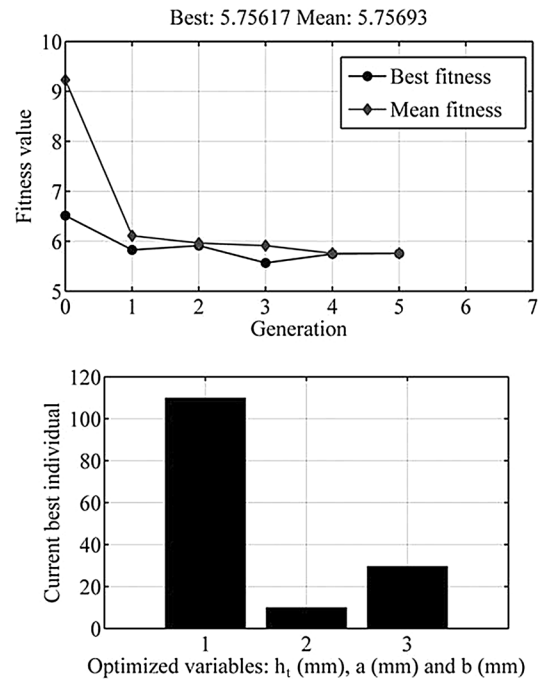


Figure 8. Optimization results—fitness value and optimized variables.

sprue well is cylinder-shaped with the base area twice as great as the one of the sprue exits and height 1.5 times higher than the one of the runner cross sections. The pouring basin was designed as offset step basin, with the aim to control both vertical and horizontal speed of the molten metal. Such design of the pouring basin allows laminar flow of the molten metal as well as the separation of slag and bubbles before metal inflow into the sprue.

Design of the Feeders

Cooling of the casting results in material shrinkage; therefore, basic function feeders are required to compensate for the metal shortage during solidification of the casting part. In contrast to filling, which is a relatively short process, feeding is a necessary, time-consuming and slow process. Cooling of the casting involves three phases of volume contraction (shrinkage)—liquid shrinkage, solidification shrinkage and solid shrinkage.²¹ Volume contraction is manifested through some adverse phenomena, i.e., internal shrinkage voids, surface deformation or dishing and surface puncture. The elimination of the above side effects is obtained by designing feeders which are removed after cooling the casting part. Casting solidification time can be predicted using Chvorinov's rule shown by the equation:

$$t_s = C \left(\frac{V}{A} \right)^2 \quad \text{Eqn. 15}$$

where t_s is the total solidification time of the part or feeder, C is a mold constant, V is the volume of metal, and A is the

total surface area of the part or feeder. As the feeder serves to compensate for the volume shrinkage in the casting part, it needs to be the final link of the solidification chain, i.e., it should be the last to solidify in directional solidification process. The longest solidification time for a given volume is the one where the shape of the part has the minimum surface area. The cylinder has the smallest surface area per volume and can easily be made, which is crucial when designing the feeder.

Namely, proposed solution is two cylindrical symmetric feeders intended to compensate for volume shrinkage of metal. It is dimensioned according to the rule that a feeder module is 20 % higher than the module of casting part, i.e., module of part which feeds.

$$\left\{ \begin{array}{l} M_{\text{feeder}} \geq 1.2 \cdot M_{\text{casting_part}} \\ C \left(\frac{V_{\text{feeder}}}{A_{\text{feeder}}} \right)^2 \geq 1.2 \cdot C \left(\frac{V_{\text{casting_part}}}{A_{\text{casting_part}}} \right) \end{array} \right\} \quad \text{Eqn. 16}$$

Optimal dimensions of the two uppermost feeders (which are open) that are identical (given the fact that they feed symmetrical halves of the casting part) are: $D = 105$ mm, $H = 80$ mm. Figure 9 shows the position of the proposed feeders.

Numerical Simulation and Implementation

In addition to practical knowledge applied in foundries, simulation programs are used to better understand the casting process and manage it more easily. The primary objective of simulation is to confirm the validity of the methodology applied in the optimization and design of the casting system and reduce the cost and ensure reliable and quality production accordingly. The entire casting process, from filling the mold cavity with liquid metal and all the way to solidification and feeding, is available as a good representation of the physical model. Computer ‘Cold Casting’ allows improving the process step by step. Geometry casting is substantially facilitated, i.e., it is easy to perform changes in the geometry of the

casting part, the position of feeder and core, etc., as well as in the parameters of the casting process (temperature of the casting part, filling speed, etc.). Model of casting part, as well as models of the optimized gating system and feeders geometry, was used in the STL graphical format.

In our paper, the alloy which is the subject of the casting simulation was not available in the software database; therefore, it was required that the data be loaded into the database. A material with chemical composition and properties similar to the one to be cast was chosen from the database. The chosen material name was changed and loaded into the user’s part of the database whereupon it was possible to load a new composition of chemical elements and features for the material to be cast. The properties of the new material remain in the database. Chemical composition of an alloy affects its castability and behavior during the casting process, as well as the properties of the final casting part.

The paper describes simulation of casting steel of chemical composition 0.5 % C, 1.4 % Mn, 0.035 % P, 0.035 % S, 0.4 % Si, 0.1 % V. Compared to standard content of chemical elements in steel (designation GS30Mn5), contents of carbon, manganese and vanadium were changed. Initial temperatures of the steel, sand mold and coldbox are 1600, 40 and 20 °C, respectively. Basic limiting conditions at casting are as follows: liquidus temperature of 1498 °C; solidus temperature of 1406 °C; criterion temperature 1: 1415.2 °C; criterion temperature 2: 1500 °C; latent heat 254 kJ/kg; feeding effectivity 30 %; surface tension coefficient 1.496 N/m.

Subsequent to defining groups and types of materials in the casting system, it was necessary to determine heat transfer coefficients—HTC for pairs of materials in contact. In sand casting mold, core surfaces are coated so as to affect thermal behavior of the mold and core. The database provides data on HTC coefficients for different material pairs. Figure 10 shows the HTC for low alloy steel and the mold

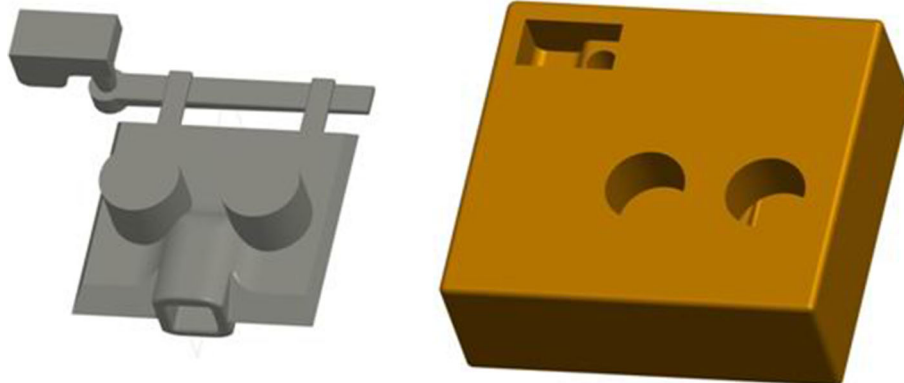


Figure 9. The proposed gating system with feeders and sand mold.

coated with a layer of a particular thickness. Other HTC coefficients applied in the simulation were used from the database software (in Sand-Core we used constant $HTC = 800 \text{ W/m}^2 \text{ K}$; in Feeder-Sand and Gate-Sand, we used the temperature-dependent Steel-Sand coefficient, whereas in Sand-Core HTC was $800 \text{ W/m}^2 \text{ K}$). Each HTC can be modified according to the specific conditions in the drive, which includes the additional thermal conductivity.

The specific heat capacity and thermal conductivity 'Lambda' are presented by graph in the temperature function in Figure 11.

Properly defined geometry network is in the basis of any simulation and is essential for the accuracy of the simulation results. The fineness and density of the network enable

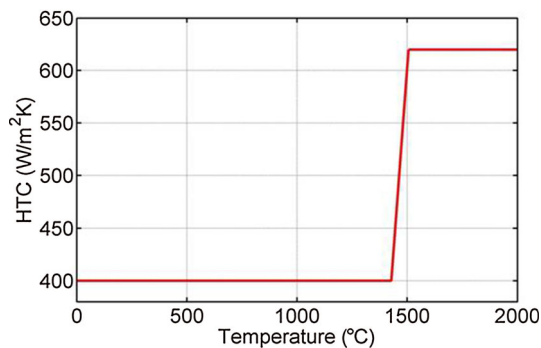


Figure 10. Heat transfer coefficient in LA-steel-coat pair.

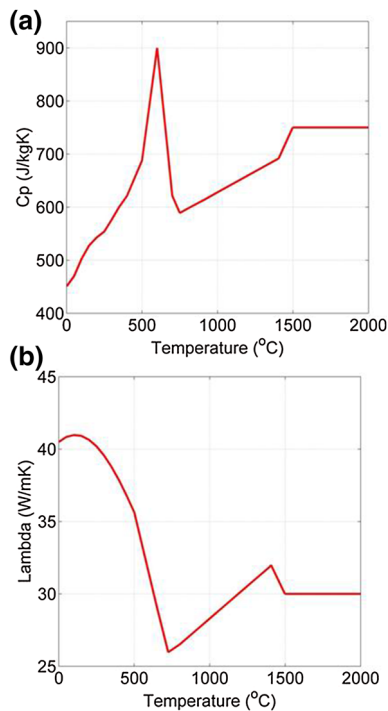


Figure 11. Material properties (a) specific heat capacity and (b) thermal conductivity.

more accurate results, but the simulation requires longer time. The total number of final volumes is one million, whereby the number of volume elements pertains to metal 157,611, without critical elements present. To bring the simulation into correlation with the physical process in reality requires at least 3 elements of network volume that are provided between two adjacent walls. In our study, the number of volumes between two adjacent walls on the axes $x/y/z$ is 154/130/49, respectively.

The simulation results provide important and essential information about the quality and correctness of the casting system. The analysis of the results of the simulation was initiated with *FSTime* criterion (which provides information on mold filling time), as its mold filling time is the subject of the optimization. Total mold filling time (casting part, gating system and feeders) is about 10 s; therefore, the result of the optimized mold filling time was in agreement with the simulation results. Another criterion is speed. Option *Velocity* provides information on the speed distribution in the casting process. Figure 12 shows that the velocity changes smoothly and uniformly according to the size of a cross section of elements of the gating system.

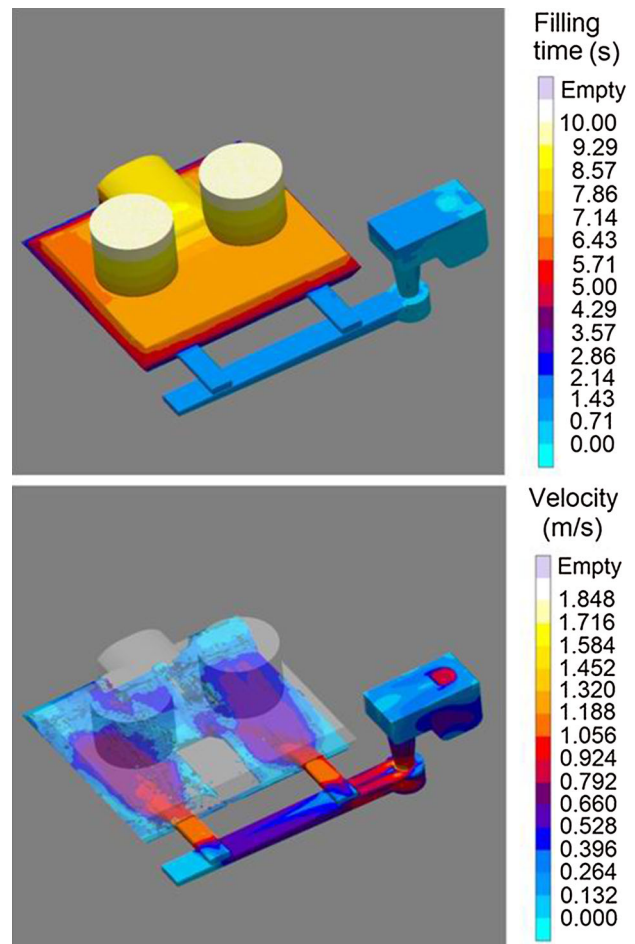


Figure 12. Mold filling time and velocity of casting.

Filling Temperature result (Figure 13) shows temperature distribution in the mold cavity, whereby the filling time is unified in a single result. This enables us to keep track of temperatures throughout the volume of the cast. Complete filling period is reduced to a single result. The values shown are based on the initial filling temperature (1600 °C).

To define solidification, i.e., cooling of the casting part, parameters and limiting conditions are required. Primarily, time or temperature at which the solidification simulation ends needs to be specified first. In our study, the final temperature in the simulation was 200 °C.

The following criteria was used to better understand thermal conditions when choosing feeders and at casting. *Feed Mod* criterion (Figure 14) was specifically designed for sand casting. The objective is to change the value of *Feed Mod* to allow directional solidification to feeders. The highest values should be in the feeder and gradually become lower in the casting part. The values of the thermal module confirmed the validity of the proposed feeders designed as based on geometric module computation.

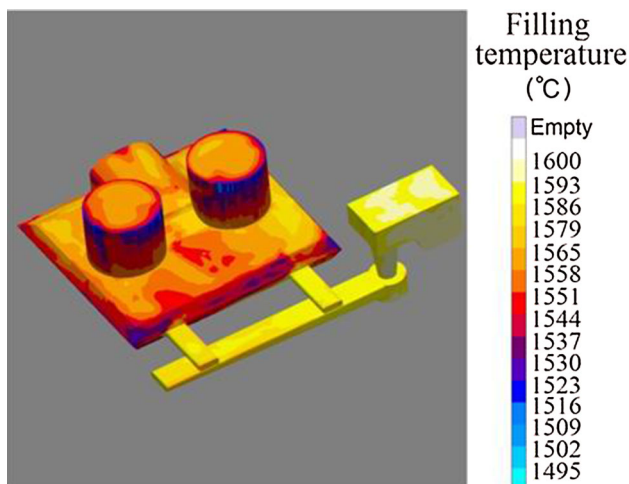


Figure 13. Temperature area in final stages of filling.

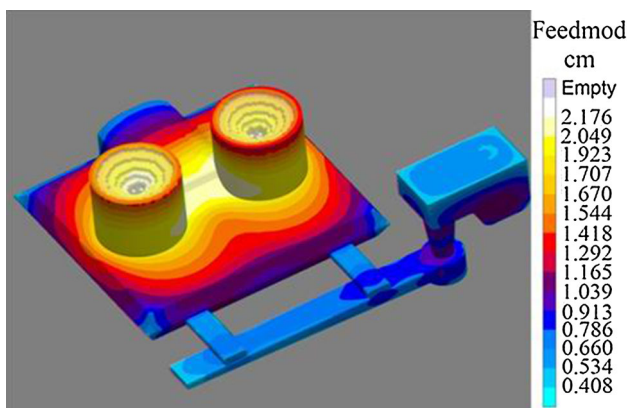


Figure 14. Feedmod criterion.

Liquidus to Solidus criterion shows time needed for a material to pass from liquid to solid state. It helps us to discover areas in the casting part that solidify later, particularly volumes which solidified after the feeding time (isolated volume). Figure 15 confirmed the correctness of the designed gating system and

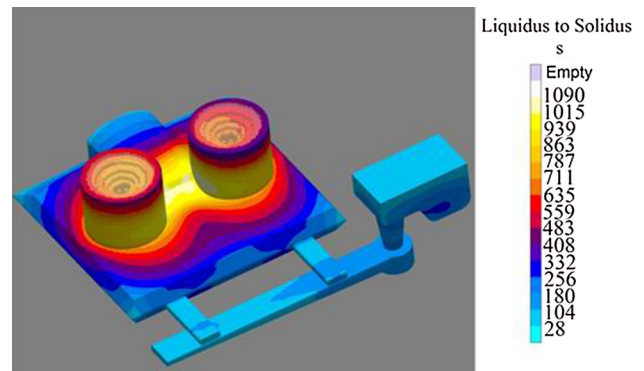


Figure 15. Time elapsed from liquidus to solidus temperature.

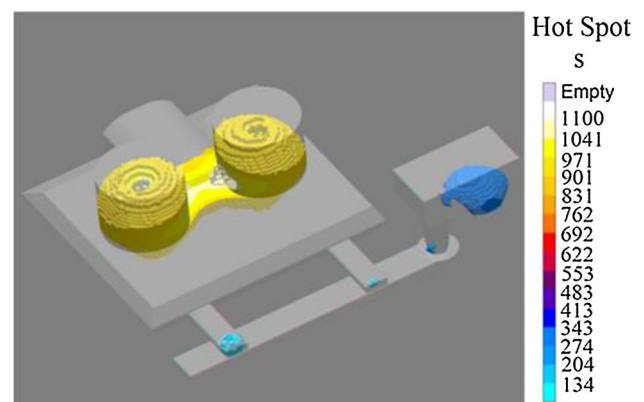


Figure 16. Hot Spot criterion.

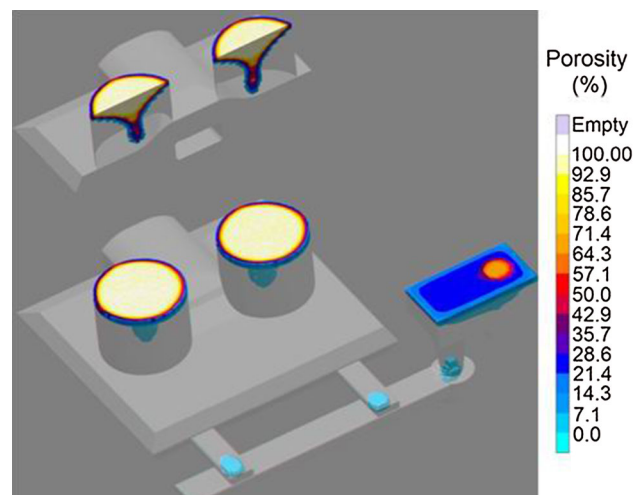


Figure 17. Porosity criterion.



Figure 18. Holder of the cutting tooth, installation and excavator bucket.

feeders by this criterion, given that the solidification period was the longest in the feeding area.

Hot Spot result shows the volumes of metals that solidify last. It helps us to identify the areas containing residual liquid metal. It also enables us to foresee possible macroscopic feeding of the volume from the feeder. Based on Figure 16, there is a volume that solidifies in the feeder, which is a prerequisite for a regular cast. *Hot Spot FSTime* shows volumes in the cast with longer solidification period. Areas defined by this criterion are still narrower than the ones defined by the *Hot Spot* result.

Total Porosity result shows cumulative porosity and microporosity in a single result, i.e., maximum values of porosity and microporosity. Figure 17 shows the X-ray total porosity in the casting part and that through the midsection of the feeder. Total porosity is expressed through percentage (%). The X-ray total porosity of the casting part renders the conclusion that alloy casting technology provides required quality.

Surface quality criterion that clearly pinpoints faults on the surface has not been explicitly defined; therefore, results from a number of different criteria are used. *Fill Tracer* is used in areas with great turbulence where lower quality of the surface due to formation of oxides is expected. As for surface quality of the casting part, it is a parameter with no particular importance in this case, given the purpose of the casting part. As the casting part is part of the system used for mining, it is the inner quality that is essential.

The proposed optimized solution of the gating system is realized in the industry. The cast part, holder of the cutting tooth, is installed on the excavator bucket. In the exploitation conditions, the holder of cutting tooth proved to be very good, as well as the entire modular solution of the excavator bucket (Figure 18).

Conclusion

The aim of this study was to present a methodology for optimizing the geometry of the gating system for the sand casting

process to maximize the filling rate based on the application of genetic algorithm. The result of the optimization is ingate cross section and casting height ($A_{\text{ingate}} = 300 \text{ mm}^2$, $h_t = 110 \text{ mm}$), obtained as a function to maximize the filling rate. Based on the study results, the optimized geometric value for each part of the gating system was defined.

Performed numerical simulations confirmed the correctness of the designed optimized gating system, in view of all the criteria. The proposed methodology of optimization provides a smooth, uniform and complete filling of the mold with pure, molten metal. Of special importance is that the methodology can be applied to parts of complex geometry, and its importance has been proven in practice, in this particular case. Generally, optimized solution of the entire casting system gave significantly better results compared to the previous casting system in terms of raising the quality of the casting part and the reduction in the consumption of molten metal.

In further research, authors will consider development of automatic pouring machines. The basic idea is the control of a total molten steel pouring system to improve the productivity of the factory, the safety of workers and the quality of the product.

Acknowledgments

The paper is the result of the work of the authors on two projects funded by the Ministry of Education and Science of Republic of Serbia: TR35037 and TR35015.

REFERENCES

1. E. Jacob, R. Sasikumar, B. Praveen, V. Gopalakrishna, *J. Intell. Manuf.* **15**, 299–305 (2004)
2. M.H. Masoumi, H. Hu, J. Hedjazi, M.A. Boutorabi, *AFS Trans.* **113**, 185–196 (2005)
3. C.E. Esparza, M.P. Guerrero-Mata, R.Z. Rios-Mercado, *Compt. Mater. Sci.* **36**, 457–467 (2006)
4. S. Guharaja, A.N. Haq, K.M. Karuppannan, *Int. J. Adv. Manuf. Technol.* **30**, 1040–1048 (2006)
5. R. Tavakoli, P. Davami, *Struct. Multidiscipl. Optim.* **36**, 193–202 (2007)

6. Z. Sun, H. Hu, X. Chen, J. Mater. Process. Technol. **199**, 256–264 (2008)
7. J. Kor, X. Chen, H. Hu, in *IEEE International Symposium on Intelligent Control* (Saint Petersburg, 2009), pp. 428–433
8. P. Kotas, C.C. Tutum, J.H. Hattel, O. Snajdrova, J. Thorborg, Int. J. Metalcast. **4**, 61–76 (2010)
9. V.D. Shinde, D. Joshi, B. Ravi, K. Narasimhan, J. Mater. Eng. Perform. **21**, 1574–1581 (2012)
10. A. Kumaravadivel, U. Natarajan, Int. J. Adv. Manuf. Technol. **66**, 695–709 (2012)
11. J.O. Oji, S.G. Datau, K.J. Akinluwade, A.T. Taiwo, D.A. Isadare, S.H. Pamtoks, A.R. Adetunji, J. Miner. Mater. Charact. Eng. **1**, 250–256 (2013)
12. B. Surekha, L.K. Kaushik, A.K. Panduy, P.R. Vundavilli, M.B. Parappagoudar, Int. J. Adv. Manuf. Technol. **58**, 9–17 (2012)
13. J.H. Holland, *Adaptation in Natural and Artificial Systems* (MIT Press/Bradford Book, Cambridge, 1992)
14. K. De Jong, in *IEEE Transactions on Systems, Man, and Cybernetics* (Springer, 1980), vol. 10(3), pp. 556–574
15. K. De Jong, in *Proceedings of the First International Conference on Genetic Algorithms and Their Applications* (Pittsburgh, 1985)
16. K. De Jong, Mach. Learn. **3**, 121–138 (1988)
17. E.D. Goldberg, *Genetic Algorithms* (Pearson Education, Upper Saddle River, 2006)
18. B. Ravi, *METAL CASTING, Computer-Aided Design and Analysis* (Prentice-Hall, New Delhi, 2005)
19. P. Larsen, *Iron melt flow in thin walled sections cast in vertically parted green sand moulds*. Dissertation (Technical University of Denmark, 2004)
20. J. Campbell, *Complete Casting Handbook*, 1st edn. (Elsevier, Oxford, 2011)
21. ASM Handbook Committee, *ASM Metals HandBook* (ASM International, Almere, 2002)

Copyright of International Journal of Metalcasting is the property of American Foundry Society, Inc. and its content may not be copied or emailed to multiple sites or posted to a listserv without the copyright holder's express written permission. However, users may print, download, or email articles for individual use.